CLAS Drift Chamber Alignment
Technique and Results: CMU Method (1998-1999)

Robert Feuerbach[*]

18th December 2001

Abstract

We have analyzed CLAS data taken with the main torus turned off as a source of straight tracks, and determined a set of alignment parameters to specify the orientation and location of the 18 drift chamber packages. The technique converged for the electron run 8935, but failed for multiple reasons when applied to a later photon run. The resulting alignment, used from 1998 to at least the end of 2001, is presented. Ideas for how to improve upon it in future efforts are also given.

Contents

[*]feuerbac@ernest.phys.cmu.edu

I Overview of the Alignment Technique

I.A Introduction

Our goal is to determine the relative wire-to-wire positions in each CLAS drift chamber (DC), and the chamber-to-chamber positions relative to each other and to the target. It is important to determine the wire positions accurately because we have seen that for a misalignment of a few millimeters, the momentum resolution can be degraded by a factor of two or more. The precision to which the wire positions must be known is governed by the desired momentum resolution. The specified design momentum resolution was $\delta p/p \leq 0.5\%$ for a $p = 1\,\mathrm{GeV/c}$ particle[1]. Since the deviation of a track from a straight line (sagitta) goes as $\xi \propto \frac{B}{p}$, we get

$$\frac{dp}{d\xi} = \frac{p^2}{\xi_1 p_1 (B/B_1)}$$

at the reference point (ξ_1, p_1, B_1). With a 50% magnetic field, the sagitta for a $1\,\mathrm{GeV}$ track near $\theta = 30°$ is $16\,\mathrm{cm}$, yielding a $\frac{dp}{d\xi} \sim 0.62\%/\mathrm{mm}$. This suggests that it is necessary to know the hit positions along a track with a maximum uncertainty of $0.8\,\mathrm{mm}$. The local position resolution of the drift chambers is on the order of $200\,\mu\mathrm{m}$ by design.

It must be kept in mind that an offset of the geometry has a consistent effect on the measured momentum of tracks in that sector, ie. it is not a source of uncorrelated error. We will refer to the relative wire-to-wire positioning inside a single drift chamber as the internal chamber geometry. It is assumed to be fixed, and is computed from direct conversions of the design drawings and databases for the drift chambers. The external geometry is then the position and orientation of the individual drift chambers in the CLAS detector.

Using data taken with the main torus magnetic field off, straight tracks can be used to study the alignment of the drift chambers without the momentum fit and the magnetic field masking the misalignments. The ideal conditions for collecting straight track data for DC alignment would be with all magnets off and a narrow incoming beam. The closest we can come to these conditions, however, is either to use a narrow ($\sigma_b < 0.5\mathrm{mm}$) electron beam with the mini-toroid magnet on to protect DC Region One, or to use a wide ($\sigma_b \sim 3\mathrm{cm}$) photon beam with all magnets off. Data of both types have been collected and analyzed. The current (as of 17-Dec-2001) best-determination of the geometry (r3_3tor2r1nom_req1_tre.map, Oct1998) was determined with electron Run 8935. There have been problems with the analysis and use of the photon data which will be discussed below.

I.B Assumptions

The initial assumptions were:

- The internal drift chamber geometry[1] is fixed.

- Distortions of the drift chamber shape, such as twists and wire sag due to gravity, are not important at the level of this analysis.

---

[1]The relative positions and directions of the individual sense wires inside a single drift chamber sector and region.

- The Region One drift chambers have the best relative (sector-to-sector) alignment since they were constructed as a single unit, with a claimed sector-to-sector accuracy of about 0.2 mm.

A special x_vs_t calibration was not performed for these runs, which probably leads to some of the very wide residual distributions for Region Two. Region Two, which is located between the magnetic coils, was calibrated for non-zero magnetic field runs and the quality of the extrapolation of the x_vs_t function to B=0 is potentially poor.

I.C   Technique

The positions and directions of the individual sense wires within a single drift chamber unit (a given region and sector) are assumed to be fixed relative to each other - the chambers are assumed to be rigid bodies. The overall geometry can then be characterized by 6 parameters: a set of offsets (d_X, d_Y, d_Z) and rotations (rot_X, rot_Y, rot_Z) of the chambers from their design position and orientation.

Using only the DC hit information, we only have access to the position and orientation of a drift chamber relative to the others in the same sector. The sector-to-sector relative alignment was taken into account by aligning the Region Two and Region Three drift chambers to the Region One chambers, since the Region One drift chambers were assembled into a single unit with tolerances of about $200\,\mu$m.

For the first pass, Region One was used as the reference drift chambers. The straight tracks were fit at the *time-based* level to the reference drift-chamber region (Region One), and at the *hit-based* level to the un-aligned regions (Region Two and Region Three). Then, the geometrical parameters for Region Two were permitted to float in order to minimize for the hits in that region:

$$\chi^2 = \sum_{tracks} \sum_{hits} \frac{(|D_{track,hit}| - |D_{hit}|)^2}{\sigma^2_{track,hit} + \sigma^2_{hit}} \tag{1}$$

where $D_{track,hit}$ is the calculated distance-of-closest approach of the track to the hit wire, D_{hit} is the drift distance returned by the x_vs_t function for that wire, $\sigma_{track,hit}$ is the uncertainty on the track position at that hit (by propagating the error matrix for the track to the hit), and σ_{hit} is the time-based resolution of the hit. The distances $D_{track,hit}$ and D_{hit} are signed according to the supposed side of the wire the track is on: $D_{track,hit}$ according to the fitted track, and D_{hit} as determined by the left-right ambiguity resolution performed over the superlayer. As the drift chamber geometry is modified by the fit, $D_{track,hit}$ is recalculated for each hit and track as the wire positions change. The **spatial residual** for a hit is $(D_{track,hit} - D_{hit})$, and is what will be examined later to determine the quality of the alignment.

After equation 1 has reached a stable minimum for Region Two, the next step is to align Region Three. The method here is similar, with this time the tracks being fit at the *time-based* level to both Region One and Two, and at the *hit-based* level to Region Three. Equation 1 is then minimized by varying the geometrical parameters for Region Three.

I.D   Track Selection and fitting Criteria

To have the minimization procedure converge to a stable result we found it necessary to:

- Select only those tracks with no more than one missing hit per superlayer per track.

- Reduce the geometric offset parameters to those accessible via the axial wires (d_X, d_Z, rot_Y).

- De-weight the stereo superlayer hits when determining the track parameters (which is performed before the alignment minimization).

- Select only those tracks containing hits within 3cm (!!) of the fitted track position.

II   Alignment Analysis with Electron Run 8935 (Oct1998)

The initial CLAS geometry was the "ideal" design geometry. An optical survey of the chambers completed on October 31, 1997 produced the first set of offsets and is called the SURVEY geometry[2]. The SURVEY offsets provided the starting geometry for the straight-track alignment analysis, and are listed in Table 3.

The DC geometric offsets used for PROD-1-9 E1 and G1A,B cooking were determined using the *empty target* B=0 Run 8935, with the CLAS_PARMS directory and DC x_vs_t calibration as it was as of 9-Sep-1998. Between 18k and 29k tracks per sector were used, depending upon the sector. The tracks were first selected with the standard CLAS tracking code, but after multiplying the σ's of the *stereo* superlayers by 100, thus deweighting them in the fit. This was done so that only the *axial* superlayers, which would later be used in the alignment fit, contributed strongly to the track parameter fit. Then, the selected tracks were fit with σ-multipliers for superlayers {1-6} of {100, 1, 4000, 4000, 7000, 7000} respectively, to fit the tracks to Region One. The overall effect was that the selected tracks were now locked in place by the Region One axial layers. Next, the projection of these tracks into Region Two were used with Eqn. 1 to align Region Two. The tracks were then re-fit to both Region One and Two, using σ-multipliers of {100, 1, 1, 100, 4000, 4000}. Again Eqn. 1 was minimized, this time to align Region Three. The final deviations of the 3 free offsets from their survey values can be found in Table 1.

To evaluate the uncertainty on these alignment parameters, we looked at their stability over multiple minimization trials, starting at different locations in the parameter space. For both Region 2 and Region 3 we found that for all sectors, δrot_Y was stable to within 0.0001 rad, and the shifts δd_X and δd_Z were stable to within 0.02 cm.

The quality of the alignment, and most importantly the change in the quality, is seen by looking at the residual distributions for the layers. These distributions were produced using Run 8936, which had a *full target* and B=0. The residual vs. layer plots for the starting survey geometry can be found Figures 1, 2, and 3. The distributions are broken down into large and small angle portions, since over a limited range of the detector the offset parameters are highly correlated. Within each given angular range, all the cells in a given layers are summed over. In the past we have found alignment offset solutions that appear to correct the residual distribution for the small angle tracks, while making the distribution for the large angle tracks much worse. As can be seen in the graphs, as one moves from one Region to the next (boundaries are at layers 13 and 19), often a jump in the center of the distribution can be seen (for example, in 1, Sector 1). These sharp jumps are caused by chamber misalignments, while the wider distributions (as can be seen in 2, Sector 4 large angle or any of the large angle plots) can be caused by a combination of the misalignment and a poor x_vs_t calibration. As was stated earlier, the x_vs_t calibration in Region Two was extrapolated to B=0 and is of questionable quality. Also, the behavior of the distributions for the small and large tracks can be quite different, hence we display their behavior separately.

After the alignment procedure, the sharp shifts in the distributions centers are, for the most part,
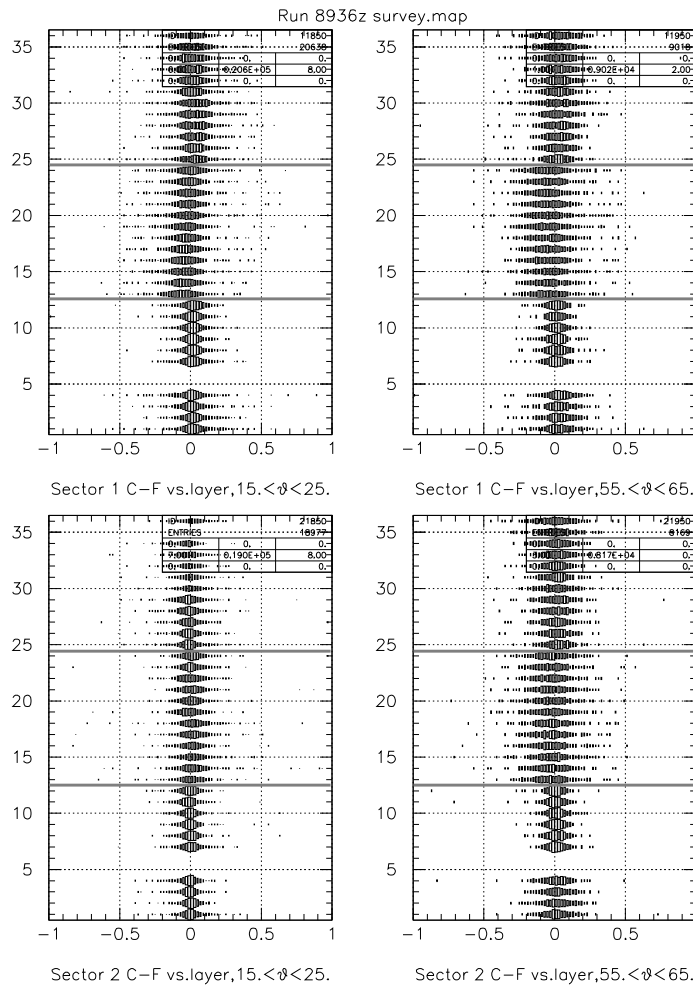
Figure 1: Sectors 1(top) and 2(bottom), spatial residual(cm) (horizontal axis) vs. layer (vertical axis) with the Survey Geometry for Run 8936(B=0), fitting to all layers. The left column contains low angle (electron) and the right large angle (proton) tracks. Layers 1 to 12 are in Region One, Layers 13-24 are in Region Two, and Layers 25-36 are in Region Three. Layers 5 and 6 do not physically exist.
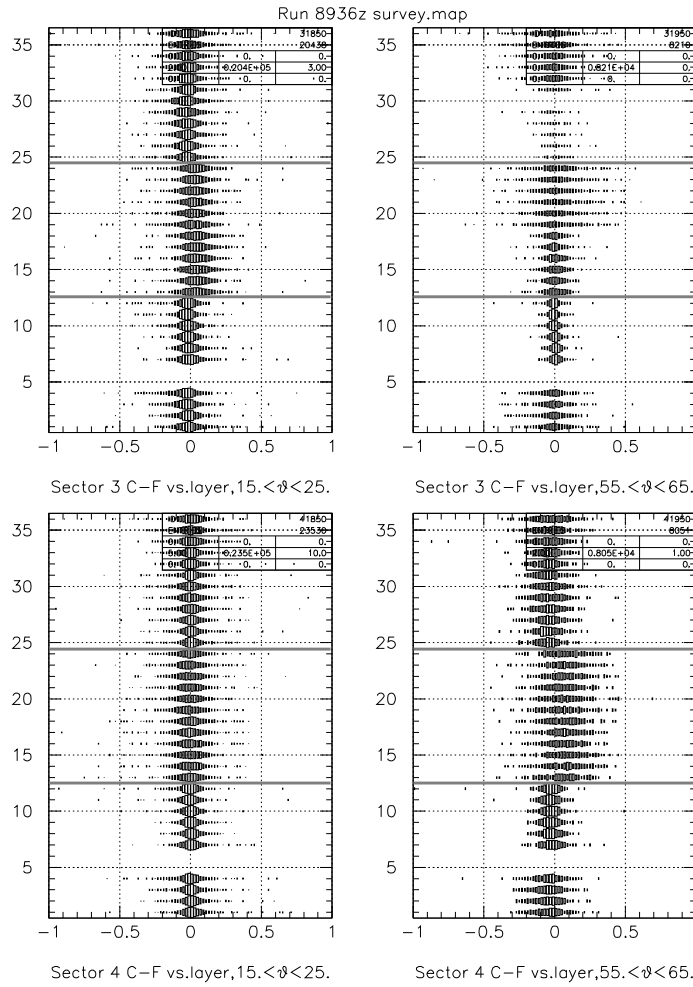
99/01/20   13.48

Run 8936z survey.map

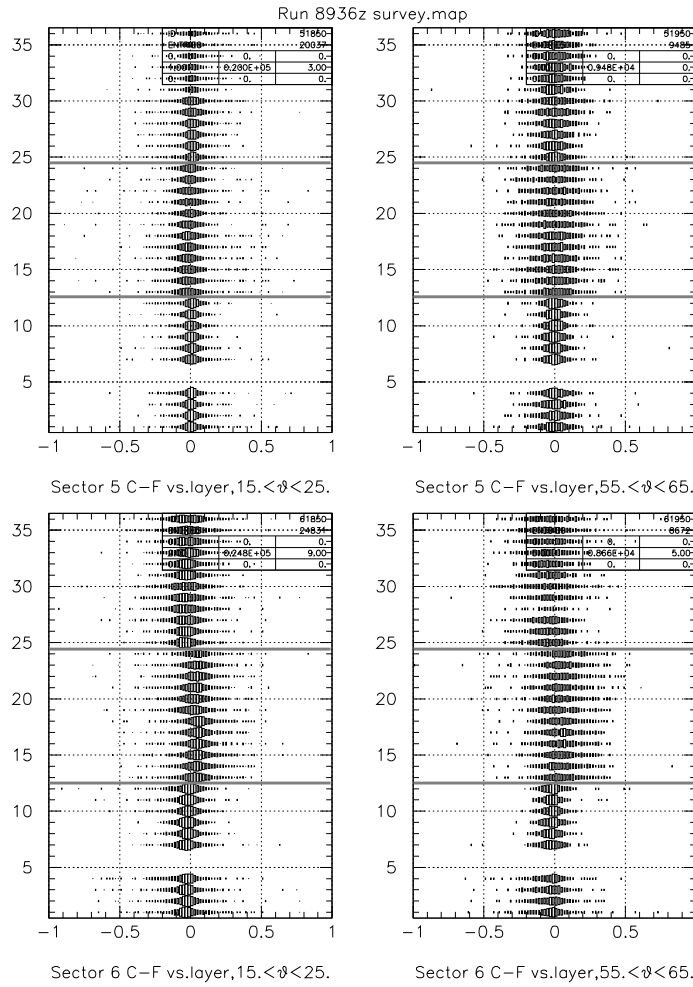Figure 2: Sectors 3(top) and 4(bottom). See caption for Figure 1.

99/01/20 13.48

Run 8936z survey.map

Figure 3: Sectors 5(top) and 6(bottom). See caption for Figure 1.

	δd_X(cm)	δd_Z(cm)	δrot_Y(rad)
Reg: 2 Sec: 1	0.1216	0.0048	-0.0001
Reg: 2 Sec: 2	0.0652	-0.0020	-0.0007
Reg: 2 Sec: 3	-0.0282	0.1022	-0.0004
Reg: 2 Sec: 4	0.0548	-0.0047	-0.0007
Reg: 2 Sec: 5	-0.0745	0.0206	0.0005
Reg: 2 Sec: 6	0.0685	-0.0727	-0.0001
Reg: 3 Sec: 1	-0.1905	0.2342	0.0009
Reg: 3 Sec: 2	-0.2145	0.2759	0.0004
Reg: 3 Sec: 3	-0.1717	0.3123	0.0003
Reg: 3 Sec: 4	-0.0216	-0.2412	-0.0007
Reg: 3 Sec: 5	-0.2997	0.1280	0.0010
Reg: 3 Sec: 6	-0.0156	-0.0332	0.0007
Uncertainty:	0.0200	0.0200	0.0001

Table 1: Deviations of the final fit parameters from the Survey offsets as determined from Run 8935. The uncertainty is the stability of the fit over multiple minimization trials.

removed, as can be seen in Figures 4, 5, and 6. The width of the residual distribution is still abnormally large for some of the Region Two chambers, probably due to the extrapolation of the x_vs_t function to B=0. The final alignment offset parameters for the Oct1998 alignment can be found in Table 4.

A more quantitative determination of the effect of the alignment procedure can be made. We compared the SURVEY and Oct1998 geometries by looking at the residual distributions summed over the axial superlayers. Again, separate distributions were collected for low angle ($15 < \theta < 25°$) and high angle ($55 < \theta < 65°$) ranges. These distributions were then fitted to a double-Gaussian function, and the results are summarized in Table 2. The parameters P2, and P3 are the primary peak center and width; and similarly are P5, and P6 for the secondary peak. While the distributions are clearly more centered after the alignment, it appears that there is still some room for improvement (see large angle Sectors 4 and 5 in Figures 17 and 19). While the widths of the distributions changed negligibly, the centroids of the primary peak, which had deviated by up to 650μm from zero, now lie within 200μm of zero, and on average are less than 150μm distant.
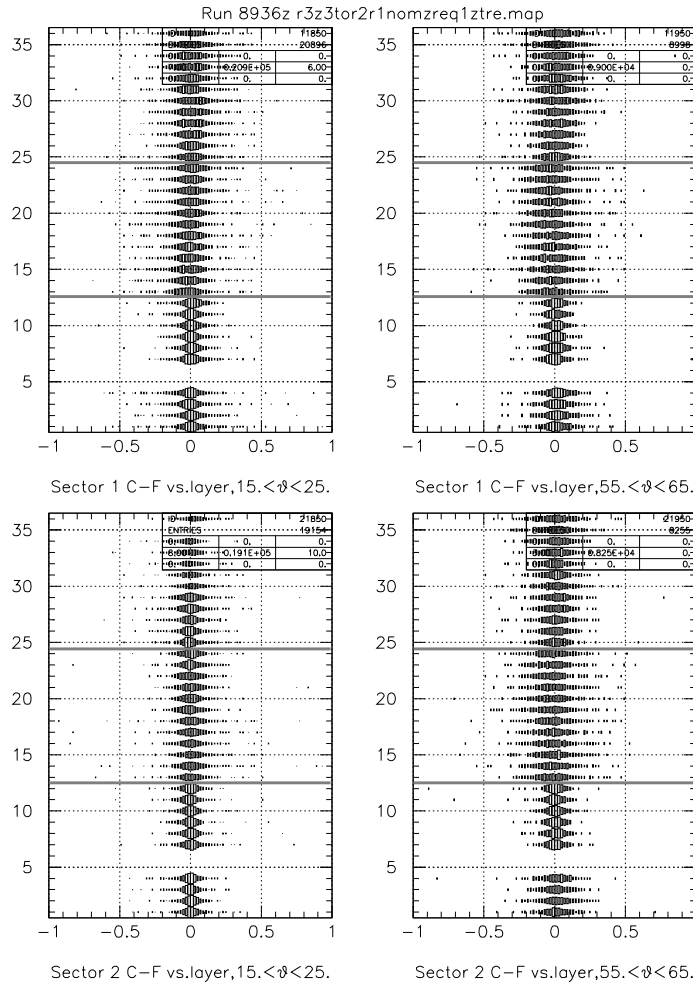
Figure 4: Sectors 1(top) and 2(bottom), residual vs. layer with the Oct1998 Geometry for Run 8936(B=0), fitting to all layers. This figure is to be compared with Figure 1.

9

99/01/21 10.33

Run 8936z r3z3tor2r1nomzreq1ztre.map

Sector 3 C−F vs.layer,15.<ϑ<25.

Sector 3 C−F vs.layer,55.<ϑ<65.

Sector 4 C−F vs.layer,15.<ϑ<25.
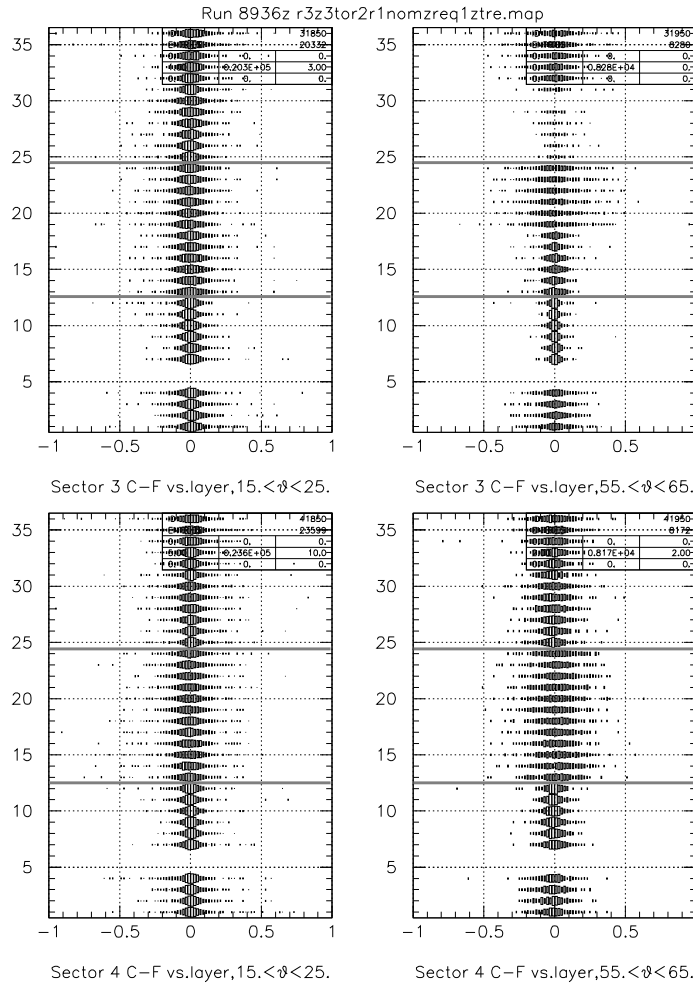
Sector 4 C−F vs.layer,55.<ϑ<65.

Figure 5: Sectors 3(top) and 4(bottom), residual vs. layer with the Oct1998 Geometry for Run 8936(B=0). This figure is to be compared with Figure 2.

10
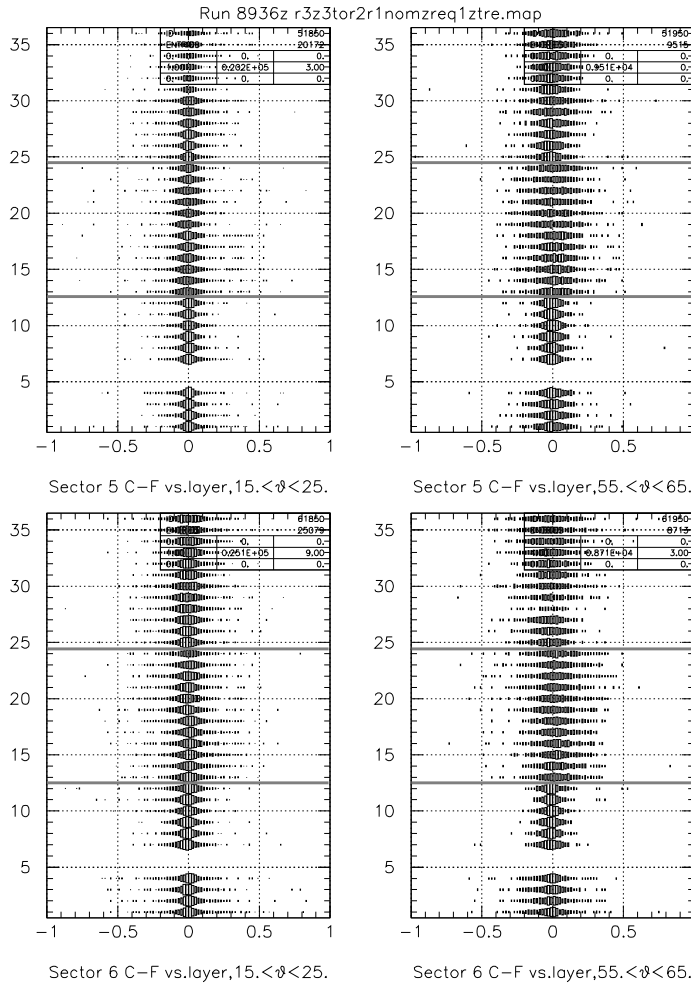
99/01/21 10.33

Run 8936z r3z3tor2r1nomzreq1ztre.map

Figure 6: Sectors 5(top) and 6(bottom), residual vs. layer with the Oct1998 Geometry for Run 8936(B=0). This figure is to be compared with Figure 3.

Sector	SL	Small Angle			Large Angle		
		$|\overline{x_{survey}}|(\mu m)$	$|\overline{x_{oct98}}|(\mu m)$	σ diff(%)	$|\overline{x_{survey}}|(\mu m)$	$|\overline{x_{oct98}}|(\mu m)$	σ diff(%)
1	2	152	32	-6	136	35	-3
	3	438	132	-9	470	177	-2
	5	303	85	2	249	54	5
2	2	37	5	-7	105	56	-6
	3	134	32	-8	263	141	-3
	5	116	48	5	174	90	-6
3	2	168	18	-5	8	7	-6
	3	393	3	-8	81	12	-23
	5	262	11	-2	124	35	2
4	2	10	26	-8	275	86	-20
	3	29	54	-4	750	194	-23
	5	21	42	-2	436	114	-7
5	2	67	6	-6	10	58	-7
	3	184	61	-7	74	173	4
	5	137	27	-2	39	92	35
6	2	198	59	-9	149	76	-16
	3	417	54	-13	283	142	-7
	5	349	78	-12	356	121	-16
Average		190	43	-6	221	92	-6

Table 2: The fit parameters for the residual distributions summed over each the axial superlayer for the SURVEY and Oct1998 DC geometries. Shown are the magnitudes of the position (ideally at 0) of the primary peak fitted position ($|\overline{X}|$) for the two geometries, and percentage change of the peak width. Note that not only do the average positions get closer to 0, but the range of values also decreases significantly. These were extracted from Figures 8-19.

III   Alignment Analysis with Photon Run 19583

A great deal of effort was put into attempting to extract a DC geometry for the Photon run 19583, taken August 1999. This run had the potential to be very useful since:

1. some Region 3 sectors of the Drift Chambers had recently been moved while being repaired;

2. the mini-toroid was not installed, so it was a true "B=0" run;

3. the target was empty, providing hard constraints on the tracks having to come from the target walls.
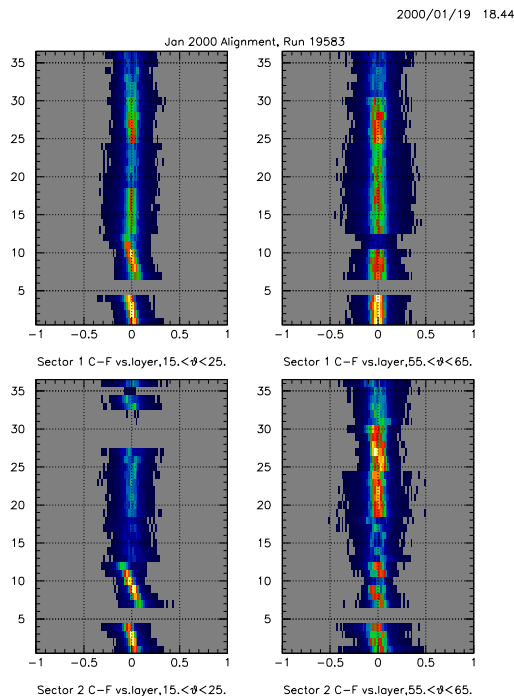

Figure 7: The residual distribution seen for Sectors 1 and 2 from the Photon run. The very strong layer dependence of the residual in Region 1 at small angles was evident in all sectors and persisted regardless of which layers were used in the fit, causing the analysis to fail.

Unfortunately, there were some problems that made this run unusable. First, it had a two-charged track trigger, but with low energy thresholds so that the data was dominated by the production of low energy e^+e^- pairs, which normally would have been swept away by the magnetic field. The low energy tracks multiple-scattered more than the higher energy hadrons (greater than 500 MeV). Secondly, the drift-time calibration of this run was very problematic, probably due to the previous issue. Lastly, we observed a layer-dependence to the track residuals in Region 1 that was not seen in any of the other data sets. This effect can be seen in the lower part of the left-hand panels of Figure 7. It is believed that this effect was due to a bug in the tracking code[5]. Another analysis using the now corrected version of the tracking library might succeed.

IV   Future Work

While we had success in improving upon the SURVEY drift chamber alignment, as has been shown in the residual distribution, there is still room for improvement. Most importantly, the chambers have been physically moved during repairs to the Region 3 drift chambers and a new software alignment has not been determined since then. Some ways to improve the current understanding of the drift chamber geometry are:

1. Improve the internal DC geometry, taking into account gravitational wire sag (at most ~150μm for 2m wire);

2. Better select high energy electrons/hadrons via $\frac{dE}{dx}$ in the EC(small angle) or TOF(very large angle) detectors;

3. Use data taken with a thin target of precisely known (x,y,z) position relative to the cryostat/R1, to supply a constraint on the track vertex position and be able to better position Region 1 inside the magnetic field.

Of course, understanding the drift chamber alignment is only a part of the issue of improving the momentum resolution of CLAS. Of equal or greater importance is to understand the magnetic field generated by the main torus. Work to parameterize the effect on the measured momentum due to both residual misalignment and magnetic field issues has been done by others[4].

V   Conclusion

We were able to analyze and use the electron run 8935 to improve the measurement of the alignment of the CLAS drift chambers. This alignment was then used for the cooking of e1b/c data with PROD-1-9 and all subsequent data sets to date. Another analysis was attempted after repairs were performed on the drift chambers, but failed due to the poor quality of the data and a bug in the tracking software. The alignment analysis can and should be repeated after every removal and re-placement of the drift chambers. We believe that the technique used here would work as well or better if applied to more recent field-off calibration runs.

Bibliography

1) M. Mestayer *et. al.,* **The CLAS Drift Chamber System**, Nucl. Instr. and Meth. A449, 81 (2000).

2) R. Feuerbach, J. McNabb, M. Mestayer, R. Schumacher, A. Skabelin, **Drift Chamber Alignment, Version 0.1**; CLAS-NOTE 98-002.

3) B. B. Niczyporuk; **Track Fitting in a Inhomogeneous Magnetic Field**; CLAS-NOTE 91-004.

4) K. Y. Kim, H. Denizli, J.A. Mueller, S.A. Dytman, **General momentum correction for for CLAS: A study of momentum corrections for the Prod 1-9 cooking of e1c data**; CLAS-NOTE 01-018.

5) Jim Mueller, University of Pittsburgh, private communication (Oct 2001).

A   The Programs

A.A   **user_align** – **Track reconstruction**

Two programs were used to do the alignment procedure. The first is a specialized user package called user_align to be used with the standard RECSIS tracking/reconstruction software. It is available under CVS at calib/dc_cal/user_align. The tracking software[3] had to be modified to permit the fitting of the zero-magnetic field data, removing the optimization of the track momentum from the fit, as well as related entries in the covariance matrix. These changes have been implemented into the standard tracking code (trk package). Other than just fitting the tracks, user_align can also:

- keep only events that contain 2 or more opposite sector tracks for electron runs (defeated with align_photon_run TCL variable);

- determine for empty target runs which target wall the tracks came from, so that it can be used as a vertex constraint in the track fitting (see align_vert_cut, trk_VXconstr, target_wall, dstmwall, upstmwall, dstmlen, and upstmlen TCL variables);

- create an NTUPLE containing hit and track information.

A sample TCL file with information as to how to use these switches can be found below.

Sample TCL file

```
#
# init file for RECSIS
#

#  load in  Tcl procedures, first check to see
#  if the user is working
#  from the stand recsis_proc.tcl or has their own

if { [file exists ../../tcl/recsis_proc.tcl] } {
    puts "Using local version of recsis_proc.tcl in ../../tcl\n";
    source ../../tcl/recsis_proc.tcl
} else {
    puts "Using standard version of recsis_proc.tcl in $env(RECSIS)/tcl\n";
    source $env(RECSIS)/tcl/recsis_proc.tcl
}

# define packages

turnoff ALL
global_section off

# set ltagger_do and lst_do = -1 for photon running
```

```
set ltagger_do  0;
set lst_do      0;
set lrf_do     -1;
set lcall_do   -1;
set ltof_do    -1;
set lcc_do     -1;
set legn_do    -1;
set lec1_do    -1;
set llac_do    -1;
set ltrk_do    -1;
set lusr1_do   -1;
set lusr0_do   -1;
set lhbid_do   -1;
set lseb_do     0;


inputfile clas_008935.A00
setc chist_filename all_layer_fit.hbook
outputfile all_layer_fit.out
setc log_file_name all_layer_fit.log
# Set the magnetic field type to 5, specifying
# that no B-field present. This is not exactly true
# for electron running, where the minitorus is present,
# but is needed to get the right switches used in
# ana_trfit.
# Besides, we don't know what the momentum of a
# particle is, so tracking it through a B-field is
# not of much use.
# Uncomment next line to force B-field=0
#set trk_magtyp 5;
set trk_print(1) 1;


#level of analysis 0: raw  2: hbt 4: tbt
set trk_level 4;


# Tbt stuff realistic curve for drift time to
# drift distance. Probably no longer needed
set dc_xvst_choice 2;


#For the ALIGNMENT, we want to be able to modify the
# SIGMA's for the track fitting
# by default, these are all = 1.
# Default running conditions
set dc_mult_Sigma(1) 1.
set dc_mult_Sigma(2) 1.
```

```
set dc_mult_Sigma(3) 1.
set dc_mult_Sigma(4) 1.
set dc_mult_Sigma(5) 1.
set dc_mult_Sigma(6) 1.

# Fit to AXIAL layers only strongly
#set dc_mult_Sigma(1) 100.
#set dc_mult_Sigma(2) 1.
#set dc_mult_Sigma(3) 1.
#set dc_mult_Sigma(4) 100.
#set dc_mult_Sigma(5) 1.
#set dc_mult_Sigma(6) 100.

# Fit to Region 1 Axial layers only strongly
#set dc_mult_Sigma(1) 100.
#set dc_mult_Sigma(2) 1.
#set dc_mult_Sigma(3) 4000.
#set dc_mult_Sigma(4) 4000.
#set dc_mult_Sigma(5) 7000.
#set dc_mult_Sigma(6) 7000.

# Fit to Region 1+2 Axial layers only strongly
#set dc_mult_Sigma(1) 100.
#set dc_mult_Sigma(2) 1.
#set dc_mult_Sigma(3) 4000.
#set dc_mult_Sigma(4) 4000.
#set dc_mult_Sigma(5) 7000.
#set dc_mult_Sigma(6) 7000.
# DO VERTEX-Constrained FIT -- empty target runs only!!!
#  align_vert_cut = 0 don't change target wall
#                   1 change target wall to either
#                     upstm or dwnstm, depending upon
#                     which has more tracks around.
#set align_vert_cut 1;
#
#  trk_VXconstr = 0  no vertex constraint on track
#                 1 or 3   constraint due to thin
#                          beam size
#                 2 or 3   constraint due to thin
#                          target (transverse to beam)
#set trk_VXconstr   2;
#
#  target_wall  =   length (thickness) of target
#                   along Z (beam direction)
```

```
#set target_wall   0.5;
#  beam_spot =  NOT USED
#set beam_spot     0.5;
#
#  dstmwall , upstmwall  = Z(cm) location of the
#                          downstream and upstream
#                          target walls. Determine
#                          location from 3-track Vertices
#set dstmwall
#set upstmwall
#
#  dstmlen, upstmlen  = distance in Z from the
#                       target-wall center the track
#                       vertex can be in order to count
#                       as a track from that wall.
#set dstmlen       0.5;
#set upstmlen      0.5;
#
# Be sure to set the TARGET POSITIONS appropriately!!!
#set TargetPos(1)   0.099920;
#set TargetPos(2)  -0.580300;
# tell FPACK not to stop if it thinks you are running
#  out of time
fpack "timestop -999999999"

# do not send events to event display
set lscat $false;
set ldisplay_all $false;

# tell recsis to pause or go
#set nevt_to_skip 10000
go 300000
setc rec_prompt "align_recsis> "
exit_pend
```

A.B aligndc – Intra-sector Alignment

The program aligndc, available under CVS at calib/dc_cal/aligndc, takes the tracks from a BOS file created with user_align and performs the actual minimization of 1 with trial DC geometries. It uses the downhill simplex method to find the minimum. The options for it are:

```
>aligndc -h
Usage:
 aligndc -o<results> [-options] <file>
        -o<results>    final fitted file of form used by dc_map
         <file>        cooked file containing B=0 tracks to be used.
Options : (default)
        -i<offsets>    offset file of form used by dc_map
        -s<sector>     list of sectors to fit coherently.
        -n<#events>    number of events to process. 0 for all (1000)
        -j<#events>    number of events to skip/jump over (0)
        -d<dim #>      dimension to fit (z,x,roty,rotx,y,rotz) (123 = z x roty)
        -l<layertype>  1 for axial, 2 for stereo, 3 for both (1)
        -rf<RegionPat> which region group to move and fit together (2)
        -M<sl><maxhole> max number of permitted holes in sl (1,2,2,2,2,2)
        -w<reg><float> factor that sigma has been multiplied by (1.,1.,1.)
        -D             debugging output flag.
        -W             turn on term weights by cos(theta) distribution.
        -P<float>      Maximum %difference between best and worst chi2.(0.000020)
```

It can accept the initial geometry offsets from either a text file in the dc_map format, or from the Map/CalDB, and it will write the output in the dc_map format to the <results> file. The input datafile of tracks <file>, generated by user_align, must contain the following BOS banks: HEAD, TBTR, TBER, and TBLA. To select which chambers to align, use the -s and -rf options; if the sector is 0, then all of Region One will be moved about as a unit (keeping it "intact"), otherwise select only one sector. Multiple Regions can be selected with -rf, and the same offsets will be applied to them. The -M option specifies the maximum number of missing hit wires for that superlayer. Also, the σ-multiplier that was used for tracking should be specified on a Region-by-Region basis with -w (for example, if Region Two was fit with a multiplier of 4000, the option would be -w24000.). The -l option specifies which superlayers will be used in the minimization.

The -W option probably should NOT be used without studying its implementation in code. It permits the user to change the weight of a track in the fit as a function of theta, to emphasize the larger angle tracks. The statistical propriety of this technique as implemented is dubious.

An example of using aligndc to align Region Two sector 2 to Region One with the (dX, dY, rotY) parameters, accounting for the σ multiplier of 4000. for Region Two, using only the *axial* superlayers, permitting a maximum number of holes per superlayer of (4,1,2,6,6,6) is:

```
> aligndc -s2 -rf2 -w24000. -d123 -l1 \
      -M14 -M21 -M32 -M46 -M56 -M66 \
      -isurvey.map -ofit_sector2-output1.map r1_8935ax.filter
```

B Geometrical Offsets

The parameter offsets for the Survey and final Oct1998 Geometries.

DC Geometry for run	2	(Survey, survey.map)				
	dX(cm)	dY(cm)	dZ(cm)	rotX(rad)	rotY(rad)	rotZ(rad)
Toroid align (xyz)	0.1310	0.0030	0.0330	0.0000	0.0000	0.0040
DC reg:1 sec:1	0.0660	-0.0940	-0.1400	-0.0008	0.0001	-0.0042
DC reg:1 sec:2	-0.0480	-0.1040	-0.1400	-0.0005	-0.0007	-0.0042
DC reg:1 sec:3	-0.1140	-0.0100	-0.1400	0.0003	-0.0008	-0.0042
DC reg:1 sec:4	-0.0660	0.0940	-0.1400	0.0008	-0.0001	-0.0042
DC reg:1 sec:5	0.0480	0.1040	-0.1400	0.0005	0.0007	-0.0042
DC reg:1 sec:6	0.1140	0.0100	-0.1400	-0.0003	0.0008	-0.0042
DC reg:2 sec:1	0.9630	0.0790	-0.1530	0.0001	-0.0001	0.0029
DC reg:2 sec:2	0.8730	0.0840	-0.1710	0.0003	-0.0001	0.0030
DC reg:2 sec:3	0.8680	-0.2160	-0.2010	-0.0003	-0.0005	0.0049
DC reg:2 sec:4	0.9300	-0.0010	-0.2170	-0.0002	-0.0007	0.0043
DC reg:2 sec:5	0.9990	0.0380	-0.2870	-0.0007	-0.0005	0.0033
DC reg:2 sec:6	0.9940	0.0410	-0.1590	0.0005	0.0003	0.0036
DC reg:3 sec:1	1.3550	-1.0950	-0.2750	0.0017	0.0007	0.0035
DC reg:3 sec:2	0.9150	0.1660	-0.1450	-0.0003	0.0007	0.0023
DC reg:3 sec:3	1.0320	0.5740	-0.1130	0.0000	0.0001	0.0038
DC reg:3 sec:4	1.1840	1.0640	0.5230	-0.0004	0.0004	0.0038
DC reg:3 sec:5	1.4150	-0.0970	0.1180	-0.0003	0.0009	0.0053
DC reg:3 sec:6	1.5750	-0.3810	0.2790	0.0001	0.0006	0.0041

Table 3: DC Geometry offsets as determined by the Survey group at Jefferson Lab.[2]

DC Geometry for run	10	**(Oct1998, r3_3tor2r1nom_req1_tre.map)**				
	dX(cm)	dY(cm)	dZ(cm)	rotX(rad)	rotY(rad)	rotZ(rad)
Toroid align (xyz)	0.1310	0.0030	0.0330	0.0000	0.0000	0.0040
DC reg:1 sec:1	0.0660	-0.0940	-0.1400	-0.0008	0.0001	-0.0042
DC reg:1 sec:2	-0.0480	-0.1040	-0.1400	-0.0005	-0.0007	-0.0042
DC reg:1 sec:3	-0.1140	-0.0100	-0.1400	0.0003	-0.0008	-0.0042
DC reg:1 sec:4	-0.0660	0.0940	-0.1400	0.0008	-0.0001	-0.0042
DC reg:1 sec:5	0.0480	0.1040	-0.1400	0.0005	0.0007	-0.0042
DC reg:1 sec:6	0.1140	0.0100	-0.1400	-0.0003	0.0008	-0.0042
DC reg:2 sec:1	1.0846	0.0786	-0.1482	0.0001	-0.0002	0.0029
DC reg:2 sec:2	0.9382	0.0838	-0.1730	0.0003	-0.0008	0.0030
DC reg:2 sec:3	0.8398	-0.2159	-0.0988	-0.0003	-0.0009	0.0049
DC reg:2 sec:4	0.9848	-0.0013	-0.2217	-0.0002	-0.0014	0.0043
DC reg:2 sec:5	0.9245	0.0382	-0.2664	-0.0007	0.0000	0.0033
DC reg:2 sec:6	1.0625	0.0407	-0.2317	0.0005	0.0002	0.0036
DC reg:3 sec:1	1.1645	-1.0939	-0.0408	0.0017	0.0016	0.0035
DC reg:3 sec:2	0.7005	0.1664	0.1309	-0.0003	0.0011	0.0023
DC reg:3 sec:3	0.8603	0.5746	0.1993	-0.0000	0.0004	0.0038
DC reg:3 sec:4	1.1624	1.0643	0.2818	-0.0004	-0.0003	0.0038
DC reg:3 sec:5	1.1153	-0.0956	0.2460	-0.0003	0.0019	0.0053
DC reg:3 sec:6	1.5594	-0.3809	0.2458	0.0001	0.0013	0.0041

Table 4: DC Geometry offsets for the Oct1998 analysis of Run 8935 (r3_3tor2r1nom_req1_tre.map).

C   Summed over SuperLayer Results

99/01/20   13.48

Run 8936z survey.map
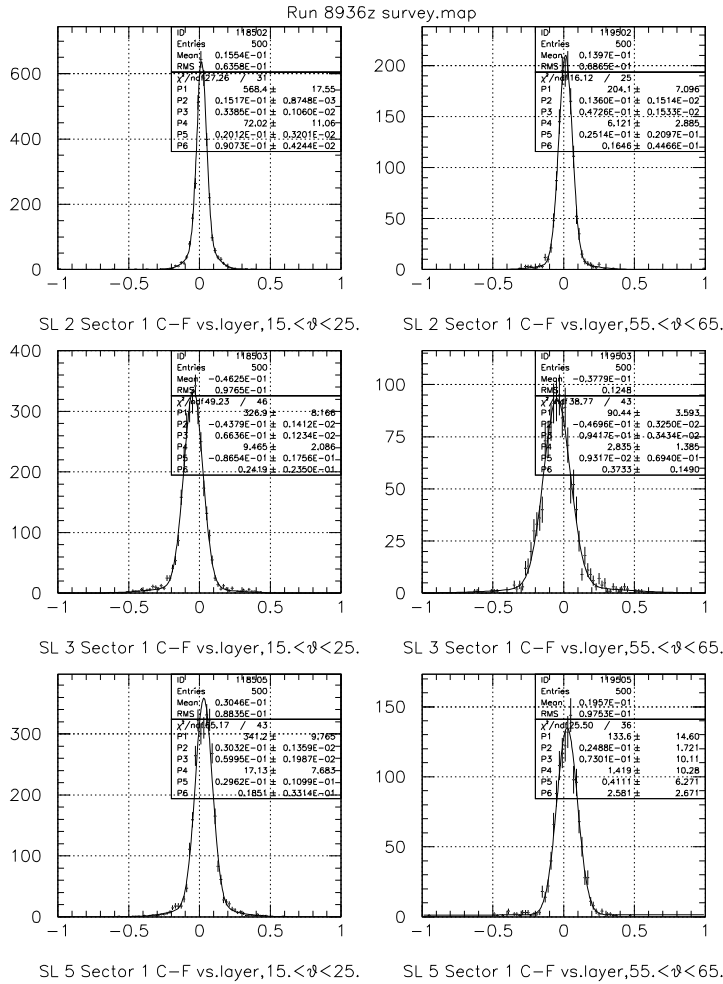
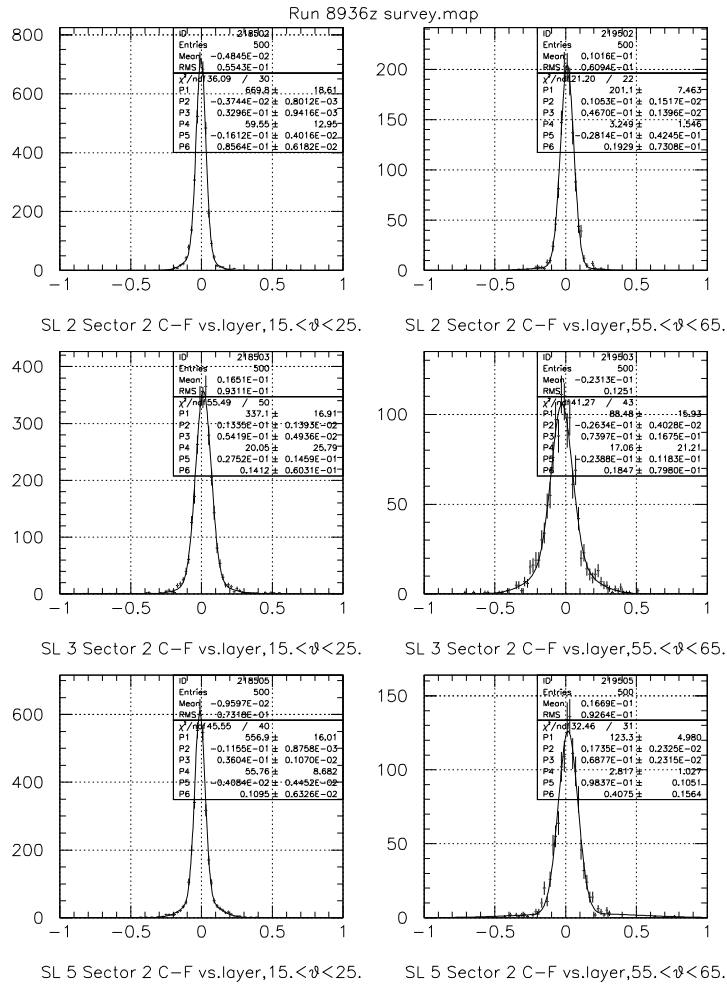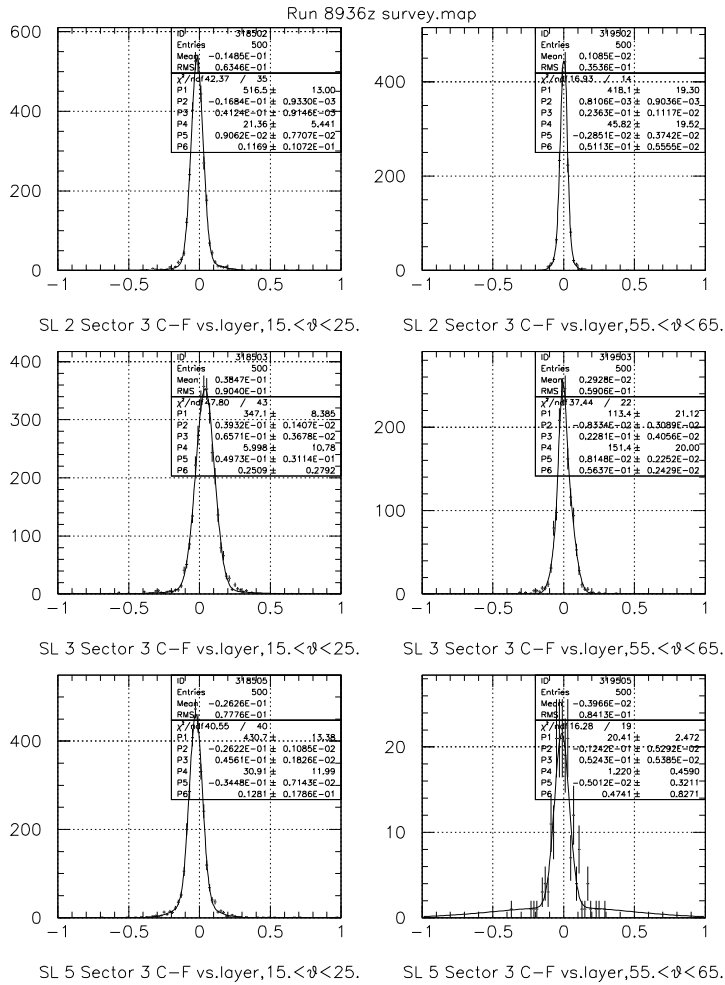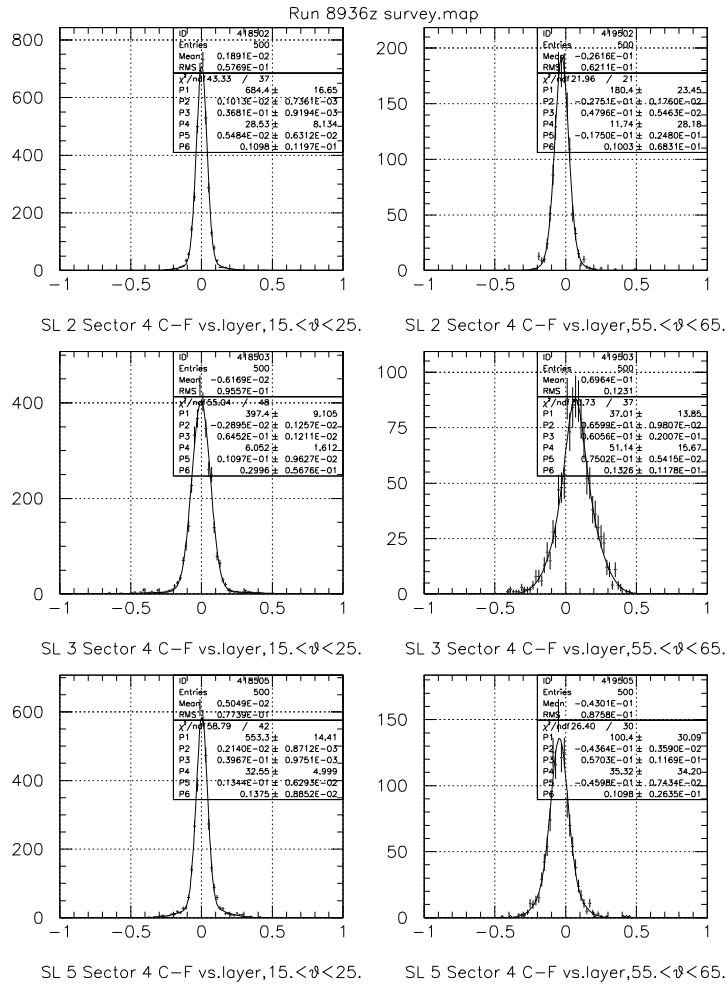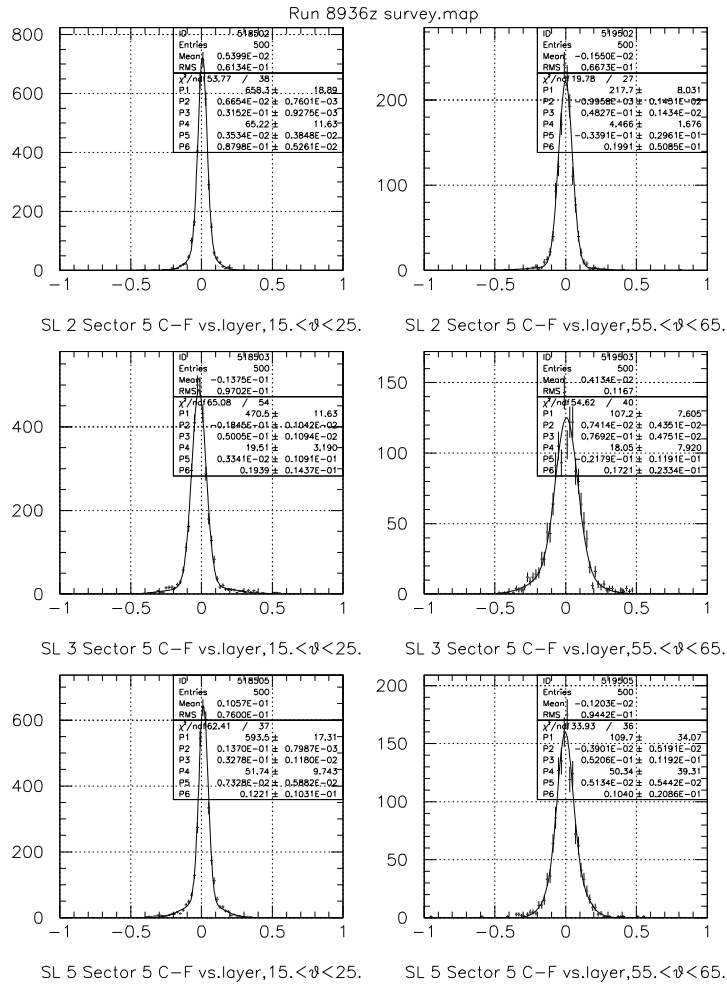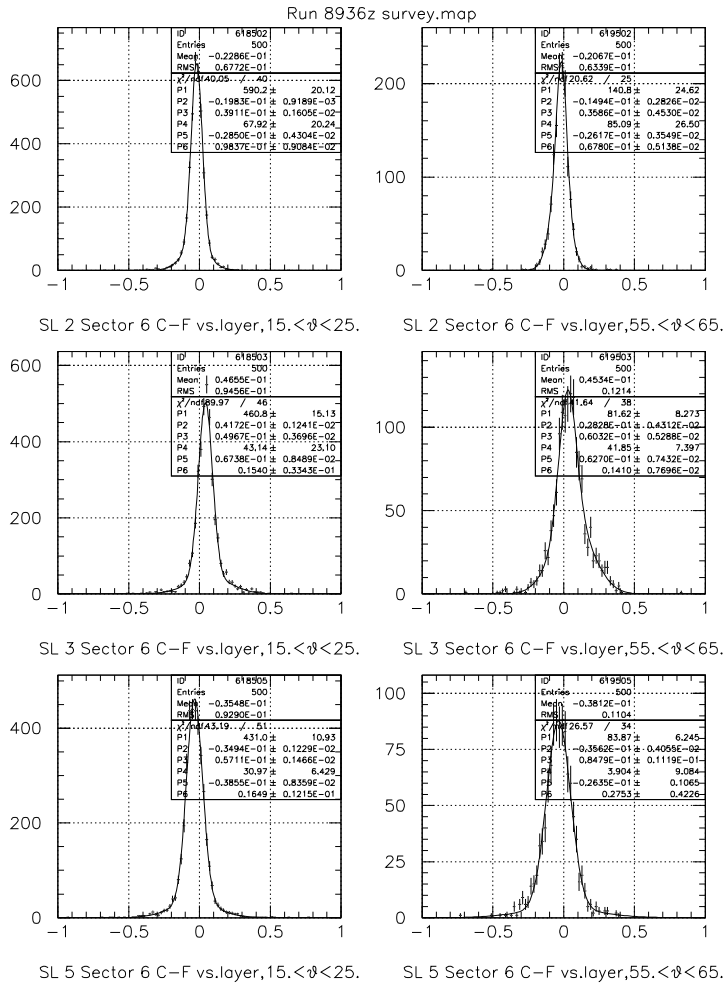Figure 8: Sector 1 spatial residual distributions for the Survey Geometry, summed over the *axial* super-layers in each region.

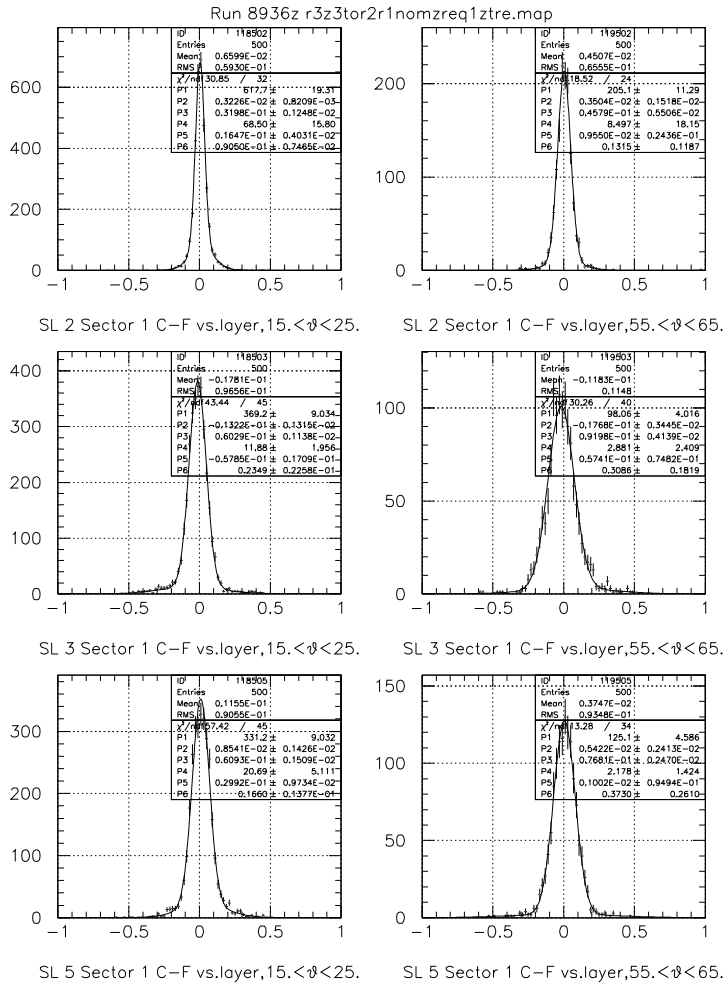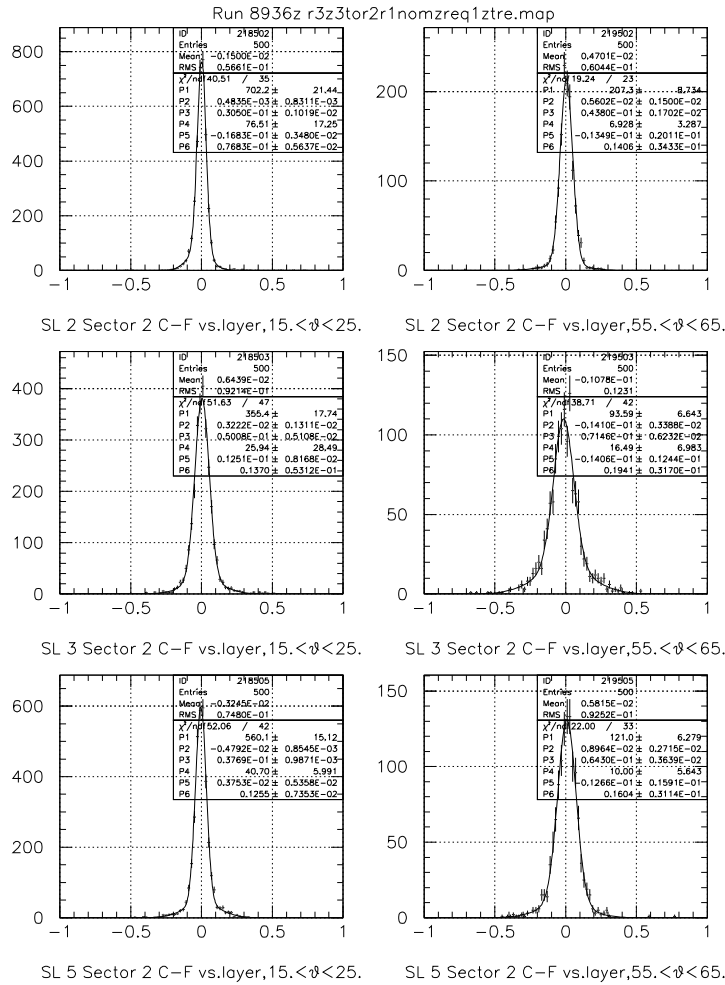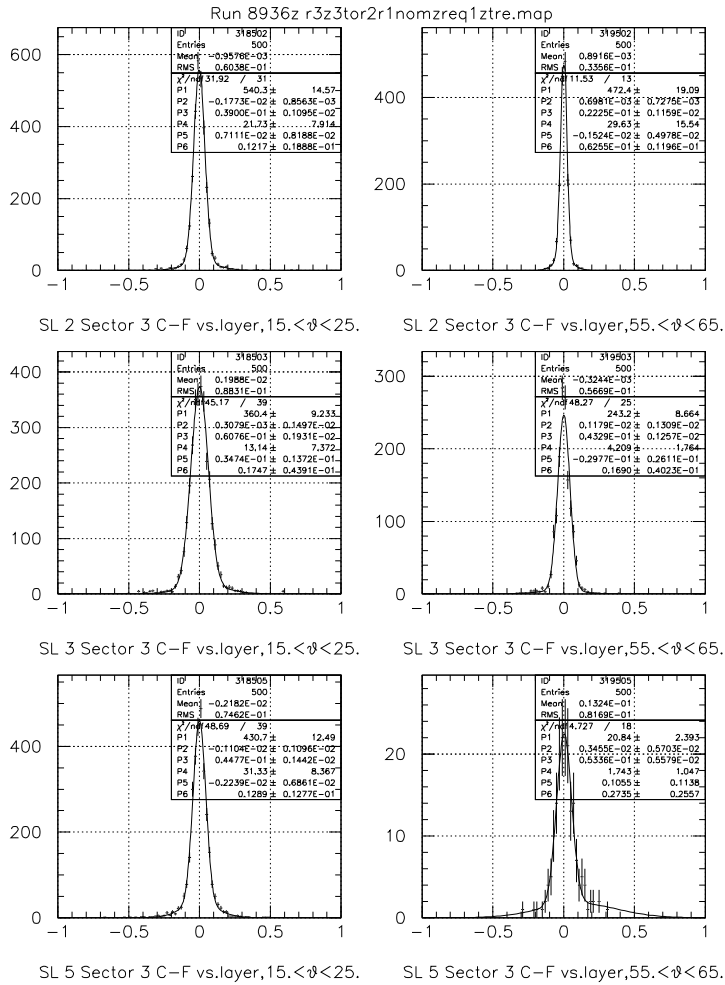Figure 9: Sector 2 spatial residual distributions for the Survey Geometry, summed over the *axial* super-layers in each region.

Figure 10: Sector 3 spatial residual distributions for the Survey Geometry, summed over the *axial* superlayers in each region.

Figure 11: Sector 4 spatial residual distributions for the Survey Geometry, summed over the *axial* superlayers in each region.

Figure 12: Sector 5 spatial residual distributions for the Survey Geometry, summed over the *axial* superlayers in each region.

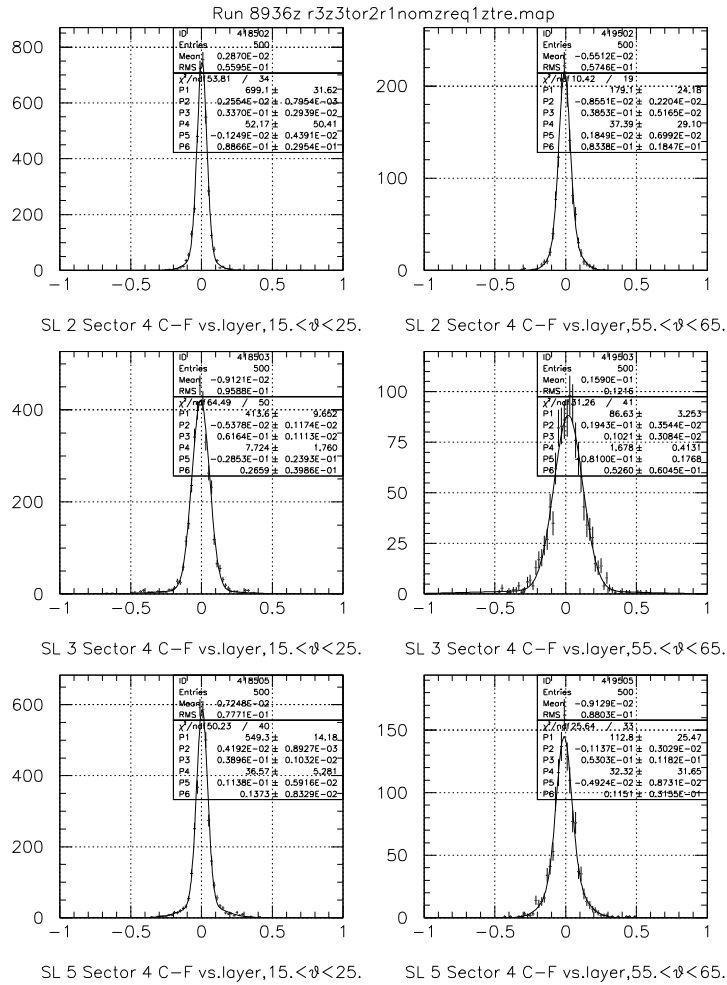Figure 13: Sector 6 spatial residual distributions for the Survey Geometry, summed over the *axial* superlayers in each region.

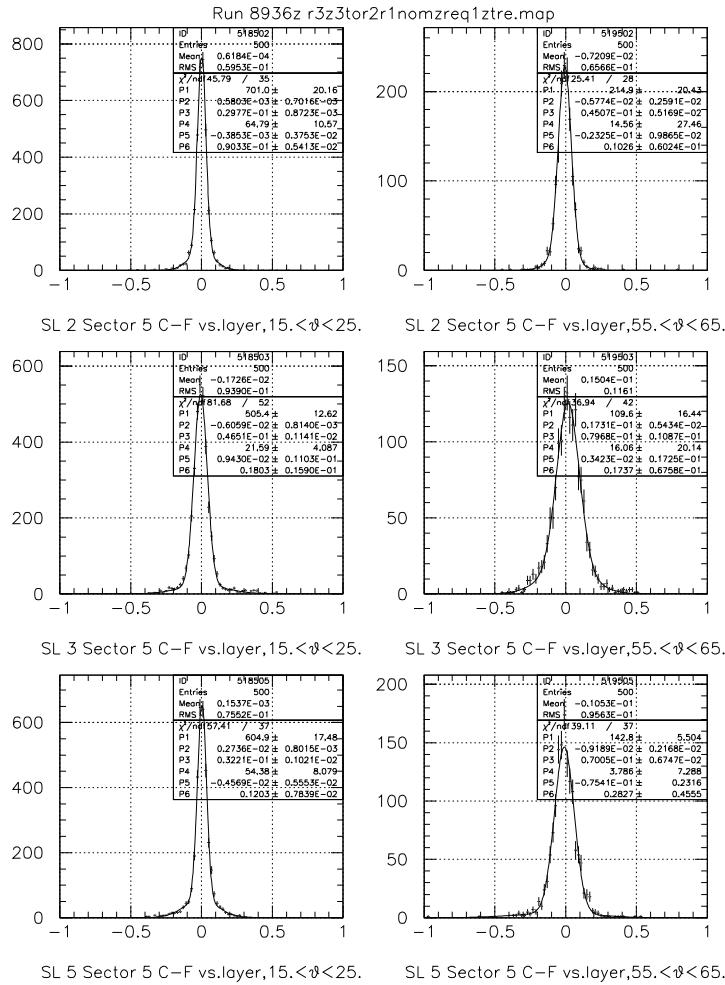Figure 14: Sector 1 spatial residual distributions for the Oct1998 Geometry, summed over the *axial* superlayers in each region.

Figure 15: Sector 2 spatial residual distributions for the Oct1998 Geometry, summed over the *axial* superlayers in each region.

Figure 16: Sector 3 spatial residual distributions for the Oct1998 Geometry, summed over the *axial* superlayers in each region.

Figure 17: Sector 4 spatial residual distributions for the Oct1998 Geometry, summed over the *axial* superlayers in each region.

Figure 18: Sector 5 spatial residual distributions for the Oct1998 Geometry, summed over the *axial* superlayers in each region.
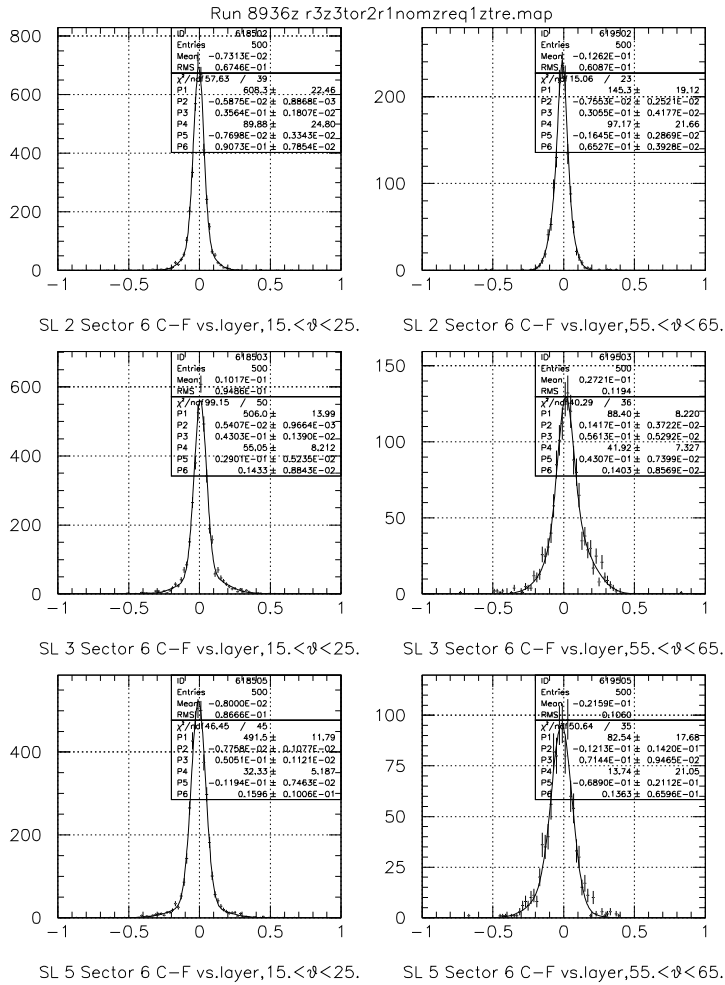
Figure 19: Sector 6 spatial residual distributions for the Oct1998 Geometry, summed over the *axial* superlayers in each region.